

# PARAMETRIC EVALUATION ON THE CURVED PART OF COMPOSITE T-JOINTS BASED ON NUMERICAL SIMULATION

**Hao Cui<sup>1,2</sup>, Yulong Li<sup>1\*</sup>, S. Koussios<sup>2</sup>, A. Beukers<sup>2</sup>**

<sup>1</sup> **School of Aeronautics, Northwestern Polytechnical University, Xian, China**

<sup>2</sup> **Faculty of Aerospace Engineering, Delft University of Technology, Delft, Netherlands**

**Keywords:** *composites, cohesive zone model, parametric evaluation, stochastic crack*

## Abstract

*A detailed numerical model is presented to predict the failure process and the strength of composite T-joint subjected to pull-off loading. The Cohesive Zone Model (CZM) is employed to simulate the delamination and crack forming in the structure, including the stochastic crack in the filler. A series of simulations are carried out to evaluate the influence of matrix, adhesive, filler (placed in the T-joints) and the radius on the strength of T-joint. The numerical results show that the nominal stiffness of the whole structure can be affected by the filler. The strength of the matrix, adhesive and filler have great impact on the loading capability, and the failure modes of the structure may change with varying the matrix, adhesive and filler material properties. Increasing the filler radius will raise the pull-off strength of T-joints. The numerical results agree reasonably with experimental results.*

## 1 Introduction

Carbon fibre reinforced composites are widely used in high performance structures that profit from their high strength, high stiffness and low weight. A number of joints are necessary to make large size structures and reduce the number

airframes and marine structures. It transfers load between two orthogonally placed members meeting at a joint. The classical T-joint is made of composite laminates curved at the root, and the radius part is inserted by filler to form a smooth transition from the T-panel to the base panel. There is growing evidence that damage in the root of the T-joints is a potential source of catastrophic failure and expensive repairs as well [1].

Various T-joints have been designed and investigated experimentally with focus on the failure modes, strength and damage tolerance [1-9]. Lotfi Ham Touché [9] and R. A. shenoi [8] have tested sandwich T-joints for marine structures. V. V. S. Rao [7] researched T-joints subjected to pull-off load and evaluated their behavior up to ultimate failure in hygrothermal environments. J. philips [1] outlined the load transfer mechanisms in single skin T-joints under representative boundary conditions, as well as the failure inception and damage progression under static loading. The T-joint region which is most susceptible to damage under both pull-off loads and three point bending loads is the radius region. Similar results have also been reported by Rispler et al [4]. K. Vijayaraju [2] found that in the case of failure initiating from the adhesive layer in the radius region, the failure progresses towards the skin/stiffener interface eventually leading to the stiffener separating from the skin.

---

\* Corresponding Author  
liyulong@nwpu.edu.cn

of components. The T-joint (or stringer stiffened skin) is a typical connection in composite

Besides experimental studies on composite T-joints, theoretical and numerical methods have been developed to analyze the load transfer mechanisms, ultimate strength levels and failure modes, in order to save experimental costs. Ege anil [3] employed Finite element analysis (FEA) to get the strain distribution in sandwich T-joints, A. Kesavan [10] and H. J. Phillips [1] conducted FEA by placing delamination of different sizes at various locations in the T-joint. F. Dharmawan [11], H. C .H. Li [12], G. Allegri [13] and Wang Man [14] have modeled composite T-joints using virtual crack closure technology (VCCT). The Mode I and II components of the strain energy release rate (SERR) were obtained by using the nodal forces and displacements. The failure loads and debonding propagation behavior was accordingly obtained. F. Dharmawan [15-16] describes some numerical methods for studying debonding in composite T-Joint using both the VCCT and CTE (Crack Tip Element) method, and proposes a modified CTE model for the T-joints. Cohesive zone models (CZM) have attracted a growing interest in the scientific community to describe failure processes and delamination in particular [17-21]. Compared to VCCT which require topological information at the crack tip, CZM is able to predict both the crack initiation and propagation. C. Balzani [22] simulated the delamination between stringer and skin in T-joints under pull-off loads using the cohesive zone model, and demonstrated the applicability of the model to predict delamination in laminated composites as well as skin - stringer separation in stiffened curved composite panels.

Parametric design and analysis methods have been used in a variety of composite applications. The finite element method has been employed to evaluate the strength and damage tolerance of composites T-joints. The effect of geometry of the T-joint on the strain distribution was investigated by Ferry Dharmawan [12]. Hawkins [27] also investigated geometry effects,

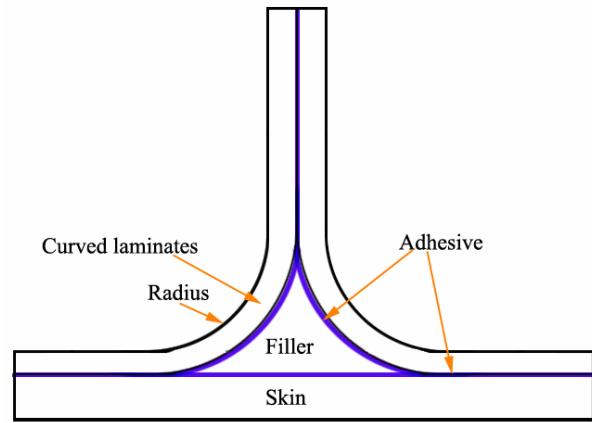


Fig.1 The geometry of T-joints

including fillet radius and over-laminate thickness for T-joints under pull-off loading, and found that increasing the radius of the fillet makes very little difference to the stiffness but significantly raises the ultimate load. Cui et al [24] performed experimental research on T-joints and compared their experimental data with theoretical results, leading to a conclusion similar to that of Hawkins. Adrian. R. Rispler [4] carried out experimental and numerical investigations of different filler placed in the root of T-joints subject to pull-off loading, and found that in some cases the T-joints with filler are weaker than the ones without filler.

Parametric studies on the failure and strength of T-joints are highly desirable. Numerical simulations are potentially the most attractive tool to evaluate the performance of such structures as they substitute costly experiments. But the numerical models presented in former works can not characterize the real structure completely since the failure of the filler at the root has not been fully simulated yet, although it has been shown that the filler has great influence on the strength and failure modes of T-joints [4].

In this paper, a detailed T-joint model incorporating failure analysis of the filler is presented. The T-joint consists of laminates, adhesive film and filler. Cohesive elements are employed to simulate delamination and crack forming. The failure mode and load-displacement curves of the T-joint are predicted under pull-off loading. Based on the

validated numerical model, a series of T-joints with different radius, material strength, and filler are simulated. The effect of these parameters on the structure performance and failure modes is then evaluated.

## 2 Numerical T-joint model

### 2.1 Cohesive zone model

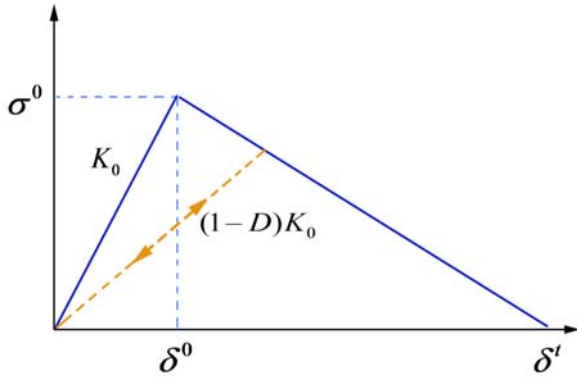


Fig. 2. Bilinear cohesive law

Cohesive elements are inserted into the interface where crack or delamination may take place. Thus a cohesive zone is bounded by upper and lower cohesive surfaces. A stress limit is set for the cohesive zone based on the material strength, which serves as a criterion for the damage initiation. That is, when the stress limit is reached, the damage starts to develop and the stress decreases with the increase of the relative displacement between these two cohesive surfaces. The element is deleted once the stress is reduced to zero, leading to the formation of a new crack area [21]. The constitutive response of cohesive element includes damage initiation and evolution. Variety of cohesive law is introduced in former research with different shape, such as bilinear, linear-parabolic, exponential and trapezoidal [18]. A bilinear cohesive law is used in this paper as shown in fig. 2, which has specific physical meaning and has been widely used.

The cohesive law is defined in terms of traction versus separation (displacement of cohesive element) curve. The bilinear cohesive law assumes initially linear elastic behavior

followed by damage initiation and stiffness degradation. Initially, the stress increases linearly with the relative displacement. The degradation begins when the stresses satisfy certain damage initiation criteria. In this paper, a quadratic nominal stress criterion is used [17-19]:

$$\left( \frac{\langle \sigma_{13} \rangle}{\sigma_{13}^0} \right)^2 + \left( \frac{\sigma_{23}}{\sigma_{23}^0} \right)^2 + \left( \frac{\sigma_{33}}{\sigma_{33}^0} \right)^2 = 1 \quad (1)$$

Here,  $\sigma_{33}^0$ ,  $\sigma_{13}^0$  and  $\sigma_{23}^0$  are the mode I, II and III

interlaminar strengths.  $\langle \rangle$  Means  $\langle a \rangle = (a + |a|)/2$ ,

hence the normal compression stress has no effect on damage. Once the element satisfies the damage initiation criteria, progressive degradation of stiffness will occur. A parameter  $D$  is introduced to represent the overall damage in the material.  $D$  evolves monotonically from 0 to 1 upon further loading after the initiation of damage. The stress components of the element are affected by the damage according to:

$$\sigma_{ij} = (1-D)\sigma_{ij}^0 \quad (i=1, 2, 3 \text{ and } j=3) \quad (2)$$

For the mixed mode, a criterion is introduced to estimate complete failure of the element after stiffness degradation:

$$\left( \frac{G_I}{G_I^C} \right)^2 + \left( \frac{G_{II}}{G_{II}^C} \right)^2 + \left( \frac{G_{III}}{G_{III}^C} \right)^2 = 1 \quad (3)$$

$G_i^C$  is the critical strain energy release rate per unit length of material under mode I loading. The element is deleted when it fulfils the damage criteria, and new crack forming or delamination takes place.

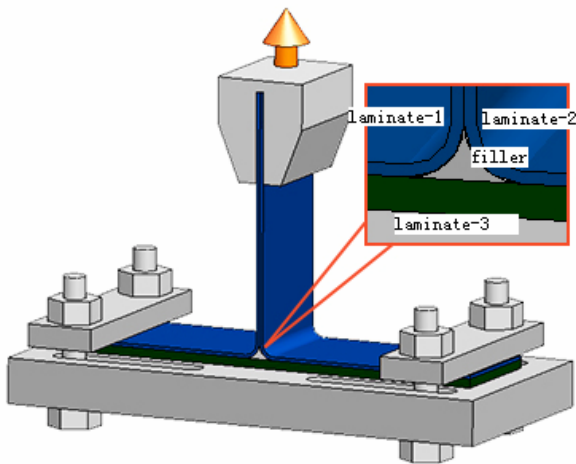


Fig.3. Sample geometry and test configuration

## 2.2 Geometry and mesh

The composite T-joint modeled here is made up of three T700/QY8911 laminates; laminate-1, laminate-2, laminate-3 are connected by adhesive at the interface as shown in figure 2. The width is 50 [mm], the length is 200 [mm] and the height is 120 [mm]. There is a curved part filled with foam at the root of the joint; the filler is attached to the laminates by adhesive bonding.

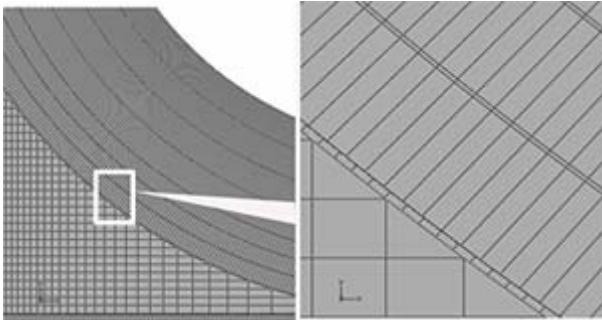


Fig. 4. Mesh in circle

The test configuration of the T-joint under pull-off loading is shown in fig. 3. The bottom of the specimen is restricted to move in the  $Y$  direction and is not permitted to rotation at any direction. The T-joint has been loaded at the head by means of prescribed displacements. Several quasi-static pull-off tests were carried out to validate the numerical simulation.

The numerical model is meshed as follows. The composite laminates are meshed by

continuum 8-node shell elements. Since initial tests have shown that delamination usually occurs at the inboard side of the laminate, layers of cohesive elements with a thickness of 0.005 [mm] are embedded between these composite layers (see in fig. 4). Delamination between these layers is allowed as a result. A layer of cohesive elements with a thickness of 0.01 [mm] is built to model the adhesive film at the interface. Then, failure of the adhesive film (debonding) is taken into analysis.

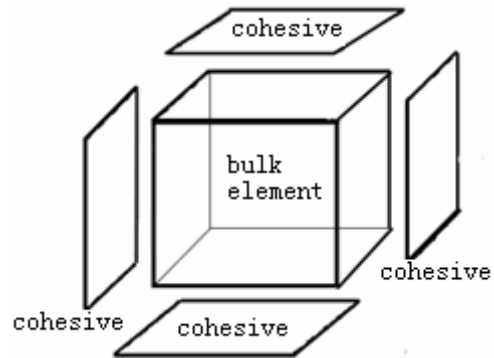


Fig. 5. Bulk element surrounded by cohesive elements

Since it is very hard to predict the crack path throughout the filler, all bulk elements in the filler are surrounded by cohesive elements to predict stochastic crack in the filler [25], as shown in fig. 5. The filler is meshed with 8-node, three-dimensional elements (C3D8); 8-node, three-dimensional cohesive elements (COH3D8) are inserted between every neighboring bulk element. These cohesive elements with high stiffness have no geometrical thickness, in order to make sure that cohesive elements will not influence the mechanical performance of filler before damage initiation.

The cohesive elements topology and node distribution are sketched in fig. 6. Node 1, 2, 3, 4 have the same coordinates. Node 1 and node 2 belong to two neighboring bulk elements, and these two elements are connected by a cohesive element with nodes 1, 2. One bulk element has different nodes with the other elements nearby, while these nodes have the same coordinates at the corresponding location. The stress is transmitted by the embedded

cohesive element. Since the cohesive elements are able to satisfy the failure criteria and can therefore be deleted, stochastic crack forming can be captured.

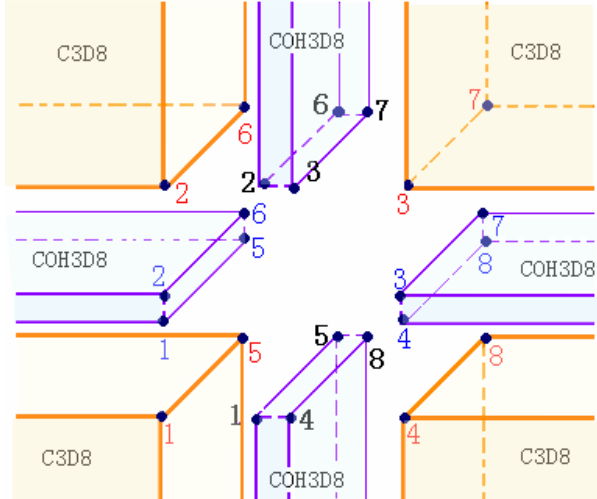


Fig.6. Nodes distribution of cohesive and bulk elements

### 2.3 Mechanical properties

The properties of the T700/QY8911 laminates are presented in table 1. Laminates 1, 2 are made of 13 layers and the overall thickness is 1.5 [mm]. The orientation of these layers are (-45/0/45/90/-45/0/90/0/45/90/-45/0/45), Laminate 3 has 32 symmetrical layers and an overall thickness of 4 [mm]. The orientation of these layers are (45/0/-45/90/0/45/0/-45/90/0/45/0/-45/0/45/-45).

The critical strain energy release rate ( $G_C$ ) of the cohesive element is deduced from the mechanical properties of resin QY8911 [26]. However, the interfacial strength has rarely been researched by experiments. Empirical approaches are often used for simulation in former research [21]. These works have shown that the interfacial strength has little influence on the obtained results [18-20]. A lower strength value is generally beneficial for improving

calculation convergence and reducing computer cost. Here, a comparatively lower strength is used as presented in table 2. The adhesive film at the interface of the laminates is made of epoxy resin QY8911. It is assumed that they have the same properties as the composite resin matrix.

The filler in the curved part is considered isotropic with  $E = 3000$  [Mpa]; the cohesive elements are assumed to have the mechanical properties as shown in table 2.

Table 1 Mechanical properties of T700/QY8911 composites

$E_{11} / MPa$	$E_{22} / MPa$	$G_{12} / MPa$	$G_{23} / MPa$	$\nu_{12}$
135000	9120	5670	5900	0.311

3 Comparison between numerical model and experiments

Several experiments for T-joints under pull-off loading have been carried out in this work, in order to validate the numerical model. Both the experimental and numerical load-displacement curves are sketched in fig. 7. Numerical results agree quite well with the experimental curves before damage initiation. The ultimate strength is nearly the same in both simulation and experiments. The structural stiffness in the simulation degrades before reaching the ultimate load; this is caused by the considerable number of cohesive elements that have already shown stiffness degradation (see FEM-1 in fig.7). The point where the structure stiffness reduces is postponed while increasing the strength of the cohesive elements by a factor of 1.5 and keeping the fracture toughness constant (see FEM-2 in fig.7). However, the structure load carrying capacity has no distinct improvement, which implies that the critical strain energy release rate is the key parameter for cohesive elements in numerical simulations rather than the strength. It

Table.2 Mechanical properties of cohesive elements

$E_{11} / MPa$	$G_{13} / MPa$	$G_{23} / MPa$	$t_n^0 / MPa$	$t_{s/11}^0 / MPa$	$G_{IC} / J \cdot mm^{-1}$	$G_{IIC} / J \cdot mm^{-1}$
3000	1150	1150	10	15	0.252	0.665

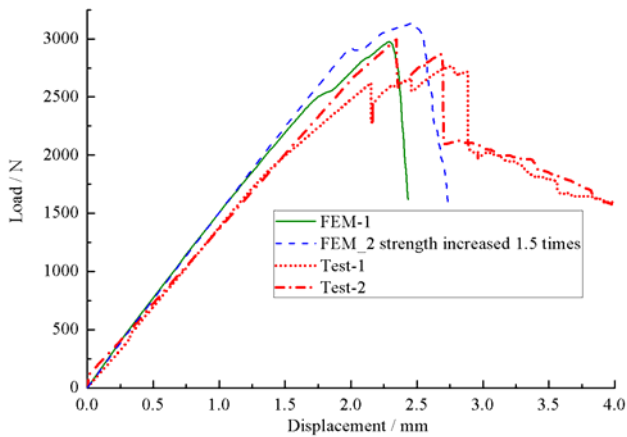


Fig.7. Load-displacement curve of composite T-joint

is expectable to get a valid result using the strength value that is defined empirically. The loading capacity drops sharply at a certain load level due to visible crack forming during both the simulation and tests. The numerical curve differs from the experiments after damage occurrence. The experiments show that the T-joint is still able to provide a relatively high loading capacity after damage. The loading capacity even increases and gets higher than the undamaged part in Test-1. However, there is no such step in the simulation. The fracture surface of the specimen can be employed to explain this difference. Fracture propagates mainly in the form of delamination and cracks in the resin at the initial phase of the failure process, which can be modeled by cohesive element very well. But the failure process becomes very complex as the fracture propagates. Effects like fibre bridging and rupture during fracture can not be taken into account in the current finite element model.

The failure process of the T-joint is presented in fig. 8. The crack appears at the top of the radius firstly, and propagates along the adhesive layer at the interface. The crack transfers into the filler and then develops downwards until reaching the bottom. Horizontal cracking occurs at the interface between filler and laminate-3, which triggers the final failure of the structure. The simulation agrees with the experiments quite

well. It can be concluded that the numerical model presented in this paper is able to simulate the failure modes and fairly predict the ultimate loading capacity of at least the composite T-joints considered here.

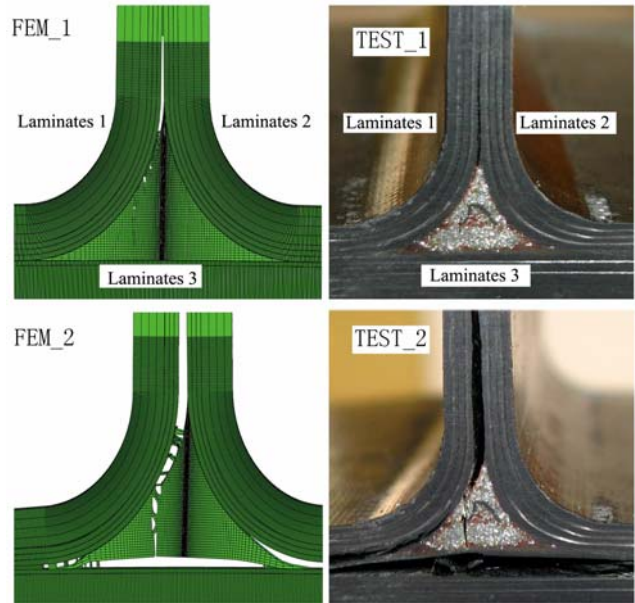


Fig.8. Failure mode of Composite T-joint under pull-off load

#### 4 Parametric evaluations

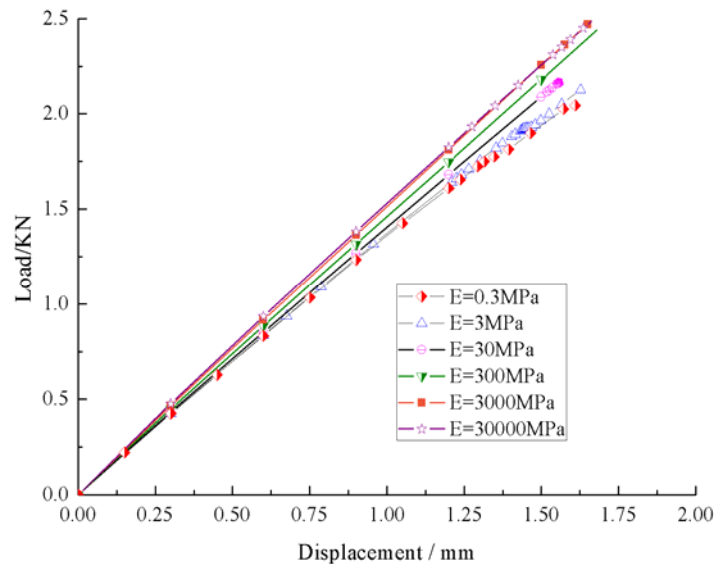


Fig.9 Linear part of load-displacement curve

#### 4.1 Influence of filler on the stiffness

The overall stiffness of T-joints is evaluated by employing fillers with different

stiffness while the thickness of the curved laminates remains 1.625 [mm], and the circle radius is 3 [mm]. The load-displacement curves before ultimate load are presented in fig. 9, from which the stiffness of T-joints can be quantified and compared with each other. The overall stiffness increases with the filler stiffness. However, the pull-off stiffness of the T-joint is nearly the same when the Young's modulus of the filler is 0.3 [MPa] and 3 [MPa]. Similarly, the overall stiffness is almost the same when the Young's modulus of the filler is 3000 [MPa] and 30000 [MPa]. It can be concluded that filler affects the stiffness of the entire T-joints at a certain extent. This influence becomes negligible when the Young's modulus of filler is lower than 3 [MPa] or higher than 3000 [MPa].

#### 4.2 Influence of filler, matrix and adhesive on the strength and failure modes

A series of simulations are carried out in which we reduce the strength and  $G_C$  of both the matrix and adhesive, while keeping the filler properties constant. Another series of simulations is carried out with reducing the strength and  $G_C$  of the filler, while keeping the properties of the matrix and adhesive constant. All the numerical results are presented in fig. 10. The performance of T-joints decreases when the matrix, adhesive or filler are weakened in terms of reduced strength and  $G_C$ ; the mechanical properties of

matrix and adhesive have more impact on the loading capacity than the filler has, which is similar to the conclusion presented by Adrian R. Rispler [4].

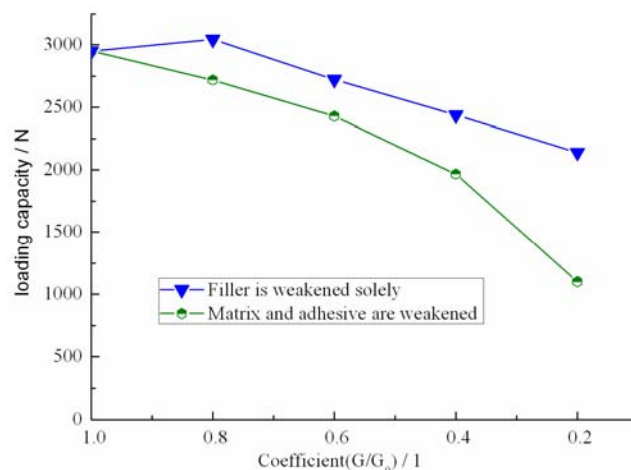
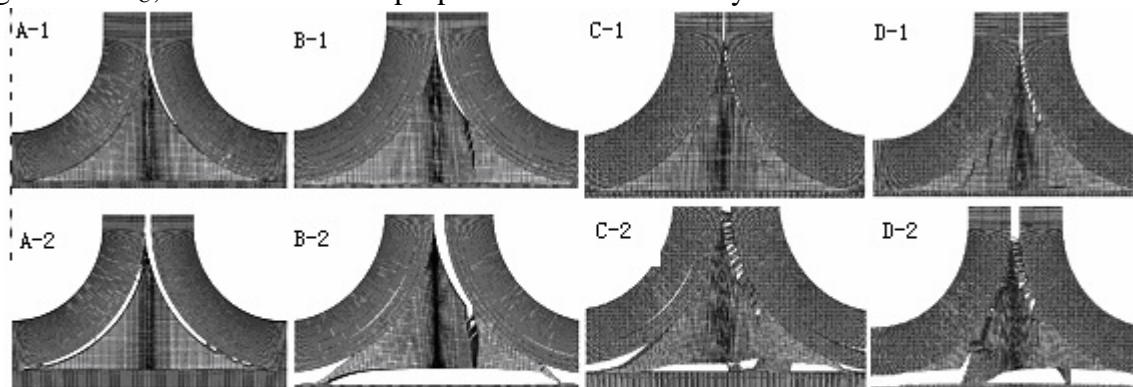


Fig.10. Loading capacity--material properties curve

Fig.11 shows different failure modes of T-joints with different material properties. It can be observed that the locations of the failure initiation are similarly right above the filler area, which is similar to the experimental results obtained by Pointer [28]. The crack propagation changes when the properties of filler, matrix and adhesive are different. The crack develops at the interface in terms of debonding when the adhesive is much weaker than the filler (A1-2 in Fig. 11). On the other hand, large scale fracture occurs in the filler when it is weaker than the adhesive film and resin matrix. The failure mode is nearly the same when the difference of



The strength and critical strain energy release rate of matrix and adhesive are reduced to 60% in A, and 80% in B, filler keeps constant; The strength and critical strain energy release rate of filler are reduced to 80% in C, and 60% in D, matrix and adhesive keep constant

Fig. 11 Failure modes of T-joint with different mechanical property of matrix, adhesive and filler

strength and  $G_C$  between resin, adhesive and filler is less than 20%. Hence, the structural configuration dominates the failure mode once the properties of each material are nearly the same.

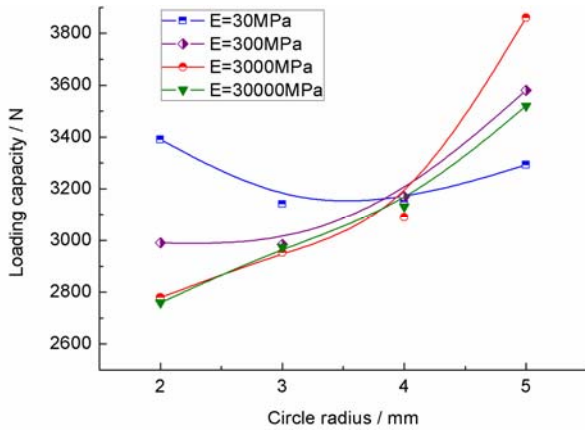


Fig.12. Loading capacity changes with the radius and stiffness of filler

### 4.3 Influence of filler stiffness and radius on the strength and failure modes

The influence of radius and filler stiffness on the strength of T-joints is also investigated in this paper. A series of T-joints with different radii and filler stiffness are simulated under pull-off loading. The pull-off strength of T-joints is presented in fig.12. The loading capacity of T-joints increases with the radius when the filler stiffness is higher than 300 [MPa], which was also concluded by Pei Junhou [29] and Hawkins [27]. However, the loading capacity has no much difference under different radii when the stiffness of the filler is low. The capacity is nearly the same at different stiffness values when the radius is equal to 4 [mm]. Hence, different filler should be used for T-joints with different radius to get the best pull-off strength.

The failure modes of T-joints with different filler are also different, as shown in fig.13. The crack initiates at both the top and bottom of the filler when the stiffness of the filler is low. The stress distribution is presented here to explain this difference. The stress at the interface between filler and laminates is very small when

the filler stiffness is low. However, the stress is quite high at the top and bottom of the filler, which cause the crack initiation. In conclusion, the stress distribution is very different between T-joint with low stiffness filler and T-joints with high stiffness filler. The filler stiffness has influence on the stress distribution in filler; the failure mode is influenced as well.

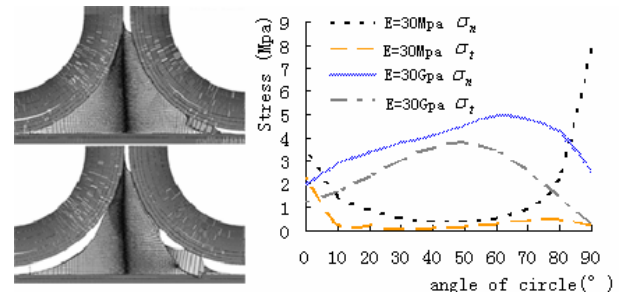


Fig. 13. The failure mode and stress distribution at the brim of filler

### 5 Conclusions

A detailed numerical model is developed in this paper to simulate the failure process of T-joints in pull off load. Delamination, debonding in the laminates and crack in the filler are incorporated in the analysis. Good agreement between numerical model and experiments can be stated. The model has been demonstrated applicable to predict a stochastic crack by forming cohesive element between every two neighboring solid elements.

Furthermore, the parametric evaluation is carried out based on this numerical model. It can be concluded that the filler stiffness influences the nominal stiffness of the whole structure at a certain extent. This influence becomes negligible when the filler is too flexible or too rigid. The strength and critical strain energy release rate of matrix, adhesive and filler have significant influence on the loading capacity and failure mode of T-joints. The pull-off strength of T-joint increases as the radius increases in most cases; this may also be influenced significantly by the filler stiffness. A larger radius may be beneficial in term of pull-off strength when the filler stiffness is higher than 300 [Mpa]; however, a smaller radius is generally better when the filler

stiffness is low.

#### References

- [1] H. J. Phillips, R. A. Sheno. Damage tolerance of laminated tee joints in FRP structures. *Composites Part A*, Vol. 29; pp 465-478, 1998.
- [2] K. Vijayaraju, P. D. Mangalgi and B. Dattaguru. Experimental study of failure and failure progression in T-stiffened skins. *Composite Structures*, Vol. 64, pp227-234, 2004.
- [3] Ege anil, Diler, Cicek.Ozes. Effect of T-Joint Geometry on the Performance of a GRP/PVC Sandwich System Subjected to Tension. *Journal of Reinforced Plastics and Composites*, Vol. 28, pp 49-57, 2009.
- [4] Adrian R. Rispler, Grent P. Steven and Liyong Tong, Failure analysis of composite T-joint including inserts. *Journal of Reinforced Plastics and Composites*, Vol. 16, pp 1642-1658, 1997.
- [5] M. D. Banea, L. F. M. da Silva. Adhesively bonded joints in composite materials: an overview, *Proc. IMechE Part L: J. Vol. 223, Materials: Design and Applications*, 2009.
- [6] Pei junhou, R.A.Sheno. Detailed research review of the performance characteristic of out of plane FRP marine structure. *Ship science report* 83, July, 1994. ISSN :0140-3818.
- [7] V. V. S. Rao, K. Krishna Veni, and P. K. Sinha. Behaviour of composite wing T-joints in hygrothermal environments. *Aircraft Engineering and Aerospace Technology*, Vol. 76, pp 404-413, 2004.
- [8] R. A. sheno, P. J .C. L. read, and C. L. Jackson. Influence of joint geometry and load regimes on sandwich tee joint behaviour. *Journal of Reinforced Plastics and Composites*, Vol. 17, pp 725-740, 1998.
- [9] Lotfi Hamitouche, Mostapha Tarfaoui and Alain Vautrin. Design and Test of a Sandwich T-Joint for Naval Ships. *Damage and Fracture Mechanics: Failure Analysis of Engineering. Materials and Structures*, 131-141.
- [10] A. Kesavan, M. Deivasigamani, S. John and I. Herszberg. Damage detection in T-joint composite structures. *Composite Structures*, Vol. 75, pp 313-320, 2006.
- [11] H.C.H. Li, F. Dharmawan, I. Herszberg and S. John. Fracture behaviour of composite maritime T-joints *Composite Structures*, Vol. 75, pp 339-350, 2006.
- [12]Ferry Dharmawa, Rodney S. Thomson , Henry Li, Israel Herszberg and Evan Gellert. Geometry and damage effects in a composite marine T-joint. *Composite Structures*, Vol 66, pp 181 - 187, 2004.
- [13]G. Allegri, X. Zhang. On the delamination suppression in structural T-fibre pinning. *Composites Part A: Applied Science and Manufacturing*, Vol. 38, pp 1107-1115, 2007.
- [14]Wang Man, Li Zecheng and Bai Ruixiang. Delamination growth characteristics for composite grid stiffened plates [J]. *Journal of Jilin University(Engineering and Technology Edition)* Vol. 01—0229—051, pp 671—5497, 2007.
- [15] F.Dharmawan, H.C.H.Li. Herszberg, S.John. Applicability of the crack tip element analysis for damage prediction of composite T-joints composite structures, Vol. 86, pp 61-68, 2008.
- [16] Dharmawan, F; John, S; Li, HCH and Herszberg, I. Damage Prediction Models for Composite T-joints in Marine Applications. *Proceedings of the 5th Australasian Congress on Applied Mechanics. Brisbane, Qld.: Engineers Australia, 2007: 775-780.*
- [17] C. Balzani, W. Wagner An interface element for the simulation of delamination in unidirectional fiber-reinforced composite laminates. *Engineering Fracture Mechanics*, Vol. 75, pp 2597-2615, 2008.
- [18] Giulio Alfano, On the influence of the shape of the interface law on the application of cohesive-zone models. *Composites Science and Technology*, Vol. 66, pp 723-730, 2006.
- [19] Paul W.Harper, Stephen R.Hallett. Cohesive zone length in numerical simulations of composite delamination. *Engineering Fracture Mechanics*, Vol. 75, pp 4774-4792, 2008.
- [20] A. Turon, C.G. Da' vila, P.P. Camanho, J. Costa. An engineering solution for mesh size effects in the simulation of delamination using cohesive zone models. *Engineering Fracture Mechanics*, Vol. 74, pp 1665-1682, 2007.
- [21] Chengye Fan, P. Y. Ben Jar and J.J. Roger Cheng. Cohesive zone with continuum damage properties for

- simulation of delamination development in fibre composites and failure of adhesive joints. *Engineering Fracture Mechanics*, Vol.75, pp 3866-3880, 2008.
- [22] W. Wagner, C. Balzani. Simulation of delamination in stringer stiffened fiber-reinforced composite shells. *Computers and Structures*, Vol. 9, pp 930-939, 2008.
- [23] Pei Junhou R. A. Sheno Examination of key aspects defining the performance characteristics of out-of-plane joints in FRP marine structures *Composites: Part A*, Vol. 27, pp 89-103, 1996.
- [24] W. C. Cui, T. Liu and J. H. Liu. Experimental Research on the Representative Connections used for MCMVs Made in GRP', China Ship Scientific Research Center Report, Wuxi, Jiangsu. 1994
- [25] Fenghua Zhou, Jean-Francois Molinari. Stochastic fracture of ceramics under dynamic tensile loading. *International Journal of Solids and Structures*, Vol. 41, pp 6573-6596, 2004.
- [26] ZHAO Qushen. Evaluation of the toughness of QY8911 bismaleimide. *Acta aeronautica et astronautica sinica*, Vol. 21, 1991.
- [27] Sheno RA, Hawkins GL. Influence of material and geometry variations on the behaviour of bonded tee connections in FRP ships. *Composites*, Vol. 23, pp 335-345, 1992.
- [28] Pointer R, J. Awerbuch and A. S. D. Wang. Evaluation of fracture / skin bond strength and durability for advanced composites fuselage crown structure. *Proceeding of the American society for composites*, 9th Technical conference, University of Delaware, pp.833-841, September 1994.
- [29] S. Kumari, P.K. Sinha. Finite element analysis of composite wing T-joints. *Journal of Reinforced Plastics and Composites*, Vol. 21, pp 1561-1585, 2002.
- permission, or have obtained permission from the copyright holder of this paper, for the publication and distribution of this paper as part of the ICAS2010 proceedings or as individual off-prints from the proceedings.

### Copyright Statement

The authors confirm that they, and/or their company or organization, hold copyright on all of the original material included in this paper. The authors also confirm that they have obtained permission, from the copyright holder of any third party material included in this paper, to publish it as part of their paper. The authors confirm that they give